

Localization driven superradiant instability

Honghao Yin,¹ Jie Hu,¹ An-Chun Ji,^{1,*} G. Juzeliūnas,^{2,†} Xiong-jun Liu,^{3,4,5,6,‡} and Qing Sun^{1,§}

¹*Department of Physics, Capital Normal University, Beijing 100048, China*

²*Institute of Theoretical Physics and Astronomy,*

Vilnius University, Saulėtekio 3, LT-10257 Vilnius, Lithuania

³*International Center for Quantum Materials, School of Physics, Peking University, Beijing 100871, China*

⁴*Collaborative Innovation Center of Quantum Matter, Beijing 100871, China*

⁵*Beijing Academy of Quantum Information Science, Beijing 100193, China*

⁶*Institute for Quantum Science and Engineering and Department of Physics, Southern University of Science and Technology, Shenzhen 518055, China*

(Dated: September 19, 2019)

The prominent Dicke superradiant phase arises from coupling an ensemble of atoms to cavity optical field when external optical pumping exceeds a threshold strength. Here we report a prediction of the superradiant instability driven by Anderson localization, realized with a hybrid system of Dicke and Aubry-André (DAA) model for bosons trapped in a one-dimensional (1D) quasiperiodic optical lattice and coupled to a cavity. Our central finding is that for bosons condensed in localized phase given by the DAA model, the resonant superradiant scattering is induced, for which the critical optical pumping of superradiant phase transition approaches zero, giving an instability driven by Anderson localization. The superradiant phase for the DAA model with or without a mobility edge is investigated, showing that the localization driven superradiant instability is in sharp contrast to the superradiance as widely observed for Bose condensate in extended states, and should be insensitive to temperature of the system. This study unveils an insightful effect of localization on the Dicke superradiance, and is well accessible based on the current experiments.

Combining cold atomic gases with cavity quantum electrodynamics [1–9] has provided a unique platform to explore exotic quantum states in atom-cavity coupling systems [10–21]. In particular, the cavity field mediates an effective long-range interaction between all atoms, and a prominent superradiant phase with the atoms absorbing and emitting the photons collectively was predicted in the notable Dicke model [22, 23]. Such superradiance transition has been achieved dynamically with a Bose-Einstein condensate (BEC) coupled to a transversely pumped optical cavity [24–28]. Furthermore, for degenerate Fermi gases inside a cavity, the superradiance with enhancement by the Fermi surface nesting was predicted [29–31], and further the topological superradiant phases were also proposed [32, 33]. These studies reveal the strong correlations between cavity photons and external center-of-mass (COM) motion of atomic assemblies in the dispersive coupling regime [8], with many exotic nonequilibrium quantum behaviors having been uncovered in these open systems [34–36].

The emergence of superradiance for BECs in a cavity is typically associated with the formation of a self-organized supersolid [24, 25]. The disordered potential, if applied to the atoms, is expected to have significant effect on superradiance. In particular, the cavity-induced incommensurate lattice can induce the Bose-glass phases in Bose-Hubbard system as the optical pumping is strong enough [37], affect localization transition of the atomic COM motion [38, 39], and lead to anomalous diffusion of the atomic wavepackets [40]. In these studies, the atoms are in ordered or extended states before the superradiance occurs. A question is, what happens if considering

the coupling of an initially localized phase to cavity?

In this letter, we investigate a BEC in a localized phase given by a one-dimensional quasi-periodical superlattice potential and coupled to a transversely-pumped optical cavity, the latter providing an effective long range interaction between the atoms. The incommensurate quasi-periodical potential can lead to the Anderson localization [41–52] and many-body localization which has attracted a considerable amount of interest recently [53–56]. In the extended regime, increasing the strength of the incommensurate potential can facilitate the tendency to the superradiant phase. Surprisingly, when the atoms enter the localized phase, we show that an unprecedented superradiant instability is driven by the resonant superradiant scatterings, for which the superradiance occurs at arbitrarily small optical pumping strength.

We consider a BEC inside a high-finesse optical cavity along the x -direction (Fig. 1). The atoms experience a one-dimensional (1D) static bichromatic incommensurate potential $V_{\text{static}}(x) = V_1 \cos^2(k_1 x) + V_2 \cos^2(k_2 x + \phi)$ obtained by superimposing two optical lattices, with ϕ a tunable relative phase, and are also illuminated by a standing-wave pumping laser with the frequency ω_p in the z -direction. The transverse confinement is sufficiently large so that the transverse motion of atoms is suppressed. In the rotating frame, the Hamiltonian reads $\hat{\mathcal{H}} = \int dx \hat{\psi}^\dagger(x) \hat{H} \hat{\psi}(x) - \hbar \Delta_c \hat{a}^\dagger \hat{a}$, where $\Delta_c = \omega_p - \omega_c$ is the detuning between the pump laser and the cavity field, $\hat{\psi}(x)$ and \hat{a} are the annihilation operators of the atom and cavity photon respectively. The full atomic Hamiltonian reads $\hat{H} = \hat{H}_0 + V_{\text{dynamic}}(x)$, with $\hat{H}_0 = -\frac{\hbar^2}{2m} \nabla^2 + V_{\text{static}}(x)$. Here $V_{\text{dynamic}}(x) = \hbar \eta (\hat{a}^\dagger +$

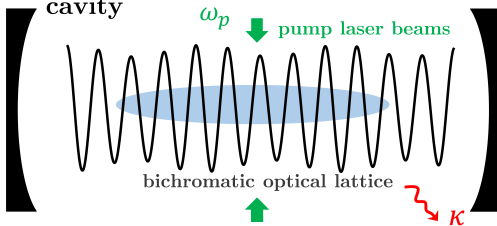


FIG. 1: A schematic diagram of the system. A 1D BEC is placed inside a high-finesse optical cavity and driven by pump laser beams counter-propagating along the z -direction. The atoms are subjected to a 1D static bichromatic potential along the x -direction, and the transverse motion of atoms is suppressed by a large transverse confinement.

\hat{a}) $\cos(k_c x) + \hbar U \hat{a}^\dagger \hat{a} \cos^2(k_c x)$ is the cavity-assisted potential, m is the atom mass and $\eta = \eta_0 \cos(k_p z_0)$ describes the transverse pumping via atoms, with $\eta_0 = g\Omega/\Delta_a$ being the strength of the interference between the pump lasers and the cavity field. Here also $U = g^2/\Delta_a$ is the atom-cavity coupling strength, $\Delta_a = \omega_p - \omega_a$ denotes the detuning between the pumping laser and atomic transition frequency ω_a , Ω is the strength (Rabi frequency) of the pumping laser, and g is the single-photon Rabi frequency of the cavity mode.

To better understand the model, we analyze first the situation without the pumping laser and the cavity field. We choose $V_1 \cos^2(k_1 x)$ ($V_1 > V_2$) as the prime lattice, and the secondary lattice $V_2 \cos^2(k_2 x)$ is relatively weaker. In the tight-binding limit, the atomic Hamiltonian $\hat{\mathcal{H}}_0$ for the bichromatic potential can be cast in the form of the Aubry-André (AA) model [41]

$$\hat{\mathcal{H}}_{AA} = -J \sum_j (\hat{c}_j^\dagger \hat{c}_{j+1} + h.c.) + \chi \sum_j \cos(2\pi\gamma j + \phi) \hat{c}_j^\dagger \hat{c}_j. \quad (1)$$

Here J is the tunneling matrix element between neighboring lattice sites and the quasirandom disorder is induced by an additional incommensurate lattice, characterized by the ratio of the lattice wave numbers $\gamma = k_2/k_1$ and disorder strength χ . For the maximally incommensurate ratio $\gamma = (\sqrt{5} - 1)/2$, the model undergoes an Anderson transition from extended to localized states at $\chi/J = 2$, beyond which all the states are localized. Such Anderson transition has been well observed for non-interacting BECs [42, 43] and photonic crystals [44]. Beyond the tight-binding limit, corrections are added to the AA model, leading to a general Aubry-André (GAA) model Hamiltonian $\hat{\mathcal{H}}_{GAA} = \hat{\mathcal{H}}_{AA} + \hat{\mathcal{H}}'$, with

$$\hat{\mathcal{H}}' = J_2 \sum_j (\hat{c}_j^\dagger \hat{c}_{j+2} + h.c.) + \chi' \sum_j \cos(4\pi\gamma j + 2\phi) \hat{c}_j^\dagger \hat{c}_j + J' \sum_j \cos\left[2\pi\gamma\left(j + \frac{1}{2}\right) + \phi\right] (\hat{c}_j^\dagger \hat{c}_{j+1} + h.c.), \quad (2)$$

where J_2 is the next-nearest-neighbor (NNN) hopping

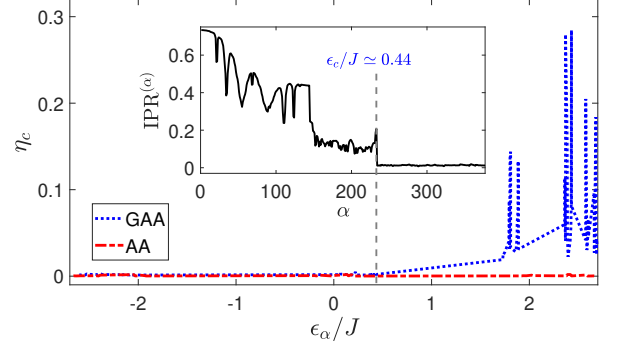


FIG. 2: The critical pumping strength η_c as a function of the energy ϵ_α/J for atoms in different eigenstates at the disorder strength $\chi/J = 2.1$ for GAA/AA model. The inset shows the inverse participation ratio (IPR) of the eigenstates in GAA model with a SPME ($\alpha \sim 233$ marked by vertical dashed line). We have chosen $U/J = 0.1$, $J'/J = -0.23$, $J_2/J = 0.072$, $\chi'/J = -0.016$ for the GAA model (blue-dotted triangle) and the corresponding AA model (red-dash-dotted circle). Other parameters are $\gamma = \frac{233}{377} \simeq 0.618$, $\gamma_c = 0.8$, and $L = 377$.

amplitude, J' and χ' are the correction parameters to the tunneling parameter J and disorder strength χ , respectively. Unlike the AA model, the GAA model may have an intermediate phase, where the localized and extended eigenstates can coexist and separated by a single-particle mobility edge (SPME) [56].

Our whole system is a hybrid Dicke and Aubry-André (DAA) model, characterizing BEC in the quasi-periodic lattice and coupled to the cavity. The dynamics of the BEC and the cavity field can be captured by the master equation $\dot{\rho} = -i[\hat{\mathcal{H}}, \rho] + \mathcal{L}\rho$ on the density matrix ρ , where $\mathcal{L}\rho = \kappa(2\hat{a}\rho\hat{a}^\dagger - \hat{a}^\dagger\hat{a}\rho - \rho\hat{a}^\dagger\hat{a})$ is a Lindblad term to describe the cavity loss with a decay rate κ . Replacing the field operator by the c-number $a \equiv \langle \hat{a} \rangle$ yields $i\partial_t a = (-\Delta_c - i\kappa + U s_1)a + \eta s_0$. Here $s_0 = \sum_j \cos(2\pi\gamma_c j) \langle \hat{c}_j^\dagger \hat{c}_j \rangle$ and $s_1 = \sum_j \cos^2(2\pi\gamma_c j) \langle \hat{c}_j^\dagger \hat{c}_j \rangle$, with $\gamma_c = k_c/2k_1$ and $\langle \hat{c}_j^\dagger \hat{c}_j \rangle$ the atomic density distribution. We seek for the steady-state solution by setting $\partial_t a = 0$, and

$$a = -\frac{\eta \sum_j \cos(2\pi\gamma_c j + \phi) \langle \hat{c}_j^\dagger \hat{c}_j \rangle}{-\Delta_c - i\kappa + U \sum_j \cos^2(2\pi\gamma_c j + \phi) \langle \hat{c}_j^\dagger \hat{c}_j \rangle}. \quad (3)$$

Note that $\langle \hat{c}_j^\dagger \hat{c}_j \rangle$ itself depends on the cavity-assisted potential, and should be determined self-consistently. In general, one can expect a transition from a “normal” state with $a = 0$ to a “superradiant” state with $a \neq 0$ by tuning e.g. the optical pumping strength η .

Figure 2 shows the numerical results of the critical pumping strength η_c versus the energy of the BEC state for the GAA/AA model. For $\chi/J = 2.1$, the GAA model gives an intermediate phase with a SPME around the energy $\epsilon_c/J \simeq 0.44$. As depicted in the inset of Fig. 2, the inverse participation ratio $\text{IPR}^{(\alpha)} \equiv$

$\sum_j |\phi_j^\alpha|^4 / (\sum_j |\phi_j^\alpha|^2)^2$ vanishes for extended states and becomes finite for localized states across the SPME. For the AA model, as $\chi/J > 2$, the system is in the localization phase with all the eigenstates being localized.

Our key observation is that an unprecedented localization driven superradiant instability of the cavity field is obtained, i.e. the cavity field emerges spontaneously for an arbitrarily small pumping strength. More exactly, whenever the BEC is in a localized state, no matter the ground state or an excited one, the superradiance can take place at a vanishing critical pumping strength. This is in sharp contrast to the extended state, where a finite pumping strength is generally required [24–28] (see also the blue-dotted line of the GAA model in Fig. 2). Since all the states in AA model with $\chi/J > 2$ are localized and not thermalizable, the superradiant instability can be obtained for the BEC with any energy within the localized band, implying that this result is insensitive to the temperature.

To gain a deeper insight to the underlying physics, we analyze the superradiant behaviour as the atomic wavefunction undergoes delocalization-to-localization transition. We take the AA model for illustration. Diagonalizing the Hamiltonian (1), we have $\hat{\mathcal{H}}_0 = \sum_\alpha \varepsilon_\alpha \hat{c}_\alpha^\dagger \hat{c}_\alpha$, with ε_α and $\hat{c}_\alpha = \sum_j \hat{c}_j \phi_\alpha^j$ being the eigenenergy and annihilation operator of corresponding eigenstate ϕ_α . The total Hamiltonian of the system can then be rewritten as

$$\begin{aligned} \hat{\mathcal{H}} = & \sum_\alpha \varepsilon'_\alpha \hat{c}_\alpha^\dagger \hat{c}_\alpha + \eta(\hat{a}^\dagger + \hat{a}) \sum_{\alpha\beta} (s_{\alpha\beta} \hat{c}_\alpha^\dagger \hat{c}_\beta + h.c.) \\ & + U \hat{a}^\dagger \hat{a} \sum_{\alpha\beta} (h_{\alpha\beta} \hat{c}_\alpha^\dagger \hat{c}_\beta + h.c.) - \Delta_c \hat{a}^\dagger \hat{a}, \end{aligned} \quad (4)$$

which leads to a series of coupled motion equations

$$\begin{aligned} i\dot{a} = & -i\kappa a - \Delta_c a + Ua \sum_{\alpha\beta} (h_{\alpha\beta} c_\alpha^* c_\beta + h.c.) \\ & + \eta \sum_{\alpha\beta} (s_{\alpha\beta} c_\alpha^* c_\beta + h.c.), \end{aligned} \quad (5)$$

$$i\dot{c}_\alpha = \varepsilon'_\alpha c_\alpha + \eta(a^* + a) \sum_\beta s_{\alpha\beta} c_\beta + U|a|^2 \sum_\beta h_{\alpha\beta} c_\beta. \quad (6)$$

Here $\varepsilon'_\alpha \equiv \varepsilon_\alpha - \varepsilon_0$ measures the eigenenergy from the lowest one ($\alpha = 0$), $s_{\alpha\beta} \equiv \sum_j \phi_\alpha^{j*} \cos(2\pi\gamma_c j) \phi_\beta^j$ and $h_{\alpha\beta} \equiv \sum_j \phi_\alpha^{j*} \cos^2(2\pi\gamma_c j) \phi_\beta^j$ denote the scatterings between α and β states. For the superradiant transition, we take that the atoms are condensed in the lowest state $\alpha = 0$, and weakly scattered to other states when cavity field emerges. In this case only the scattering terms $s_{0\alpha}$ and $h_{0\alpha}$ are relevant. We define for convenience $s_\alpha \equiv s_{0\alpha} = s_{\alpha 0}^*$ and $h_\alpha \equiv h_{0\alpha} = h_{\alpha 0}^*$. The case for atoms initially condensed in other states is similar.

Now we examine the superradiance phase transition. For the case $\chi < 2$, the wavefunctions of the states are extended, resembling the quasi-momentum states. One can find that the cavity field cannot induce self-scattering

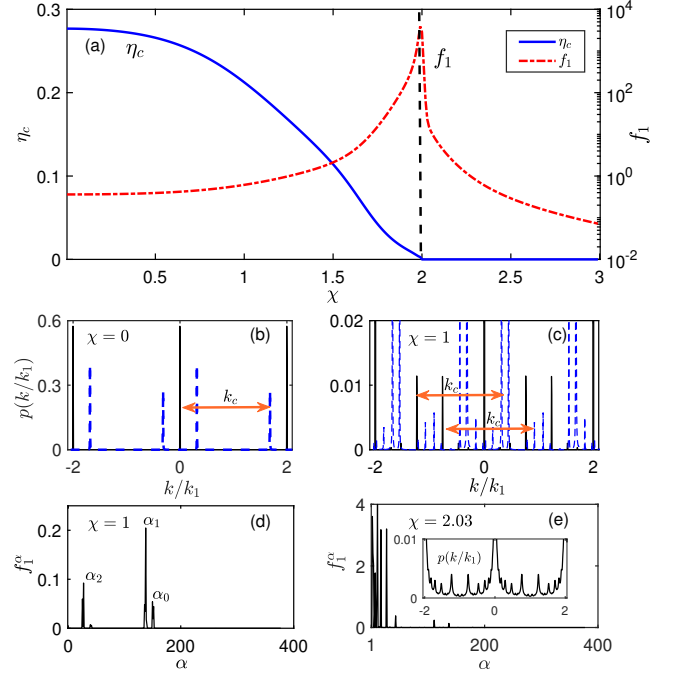


FIG. 3: (a) The critical pumping field strength η_c and the susceptibility f_1 as a function of the disorder strength χ . Here, the parameters $L = 377$, $N = 100$, $\Delta_c/J = -1$, $\kappa/J = 1$, and $\gamma_c = 4/5$. The momentum distributions of the ground state (black solid) and an excited state (blue dashed) with disorder strength $\chi = 0.0$ (b) and 1.0 (c). Susceptibility f_1^α for the disorder strength $\chi/J = 1$ (d) and $\chi = 2.03$ (e). In the latter the term f_1^0 diverges and is not plotted. The inset shows the corresponding momentum distribution of the ground state.

within the ground state and so $s_0 = 0$. The critical value of the pumping strength reads

$$\eta_c = \sqrt{\frac{1}{4Nf_1} \frac{\kappa^2 + \bar{\Delta}'_c}{-\Delta'_c}}, \quad (7)$$

with $f_1 = \sum_\alpha |s_\alpha|^2 / \varepsilon'_\alpha$, $\bar{\Delta}'_c = \Delta_c - 2UNh_0$, where $h_0 = 1/2$ gives a constant shift of cavity detuning. In the extended regime, the susceptibility f_1 is finite and the critical value of the pumping strength determined by Eq. (7) is also finite. On the other hand, Fig. 3(a) shows that as the disorder strength increases, the value f_1 increases rapidly (red curve), and the superradiance tendency is strongly enhanced, with the critical pumping field strength η_c (blue curve) decreasing significantly with increasing the disorder lattice potential. When increasing χ to the delocalization-to-localization transition point with $\chi = 2$, the susceptibility f_1 diverges and the superradiance threshold becomes zero.

The unique role played by incommensurate lattice potential on the superradiance enhancement becomes more transparent in the momentum space. For the limit case with $\chi = 0$ (no secondary disorder lattice), the momentum distribution of the ground state, $P(k/k_1) =$

$|\sum_j \phi_0^j \exp(i\pi j k/k_1)|^2$, exhibits primary peaks at $k = 0$ and $2k_1$ (equivalent to $-2k_1$) in the first Brillouin zone [43–47]. The momentum peaks of the α -th excited state are found to appear at $\pm\alpha k_1/L$ and $\pm(2-\alpha/L)k_1$, which are shifted from the primary peaks of the ground state by $\pm\alpha k_1/L$, with α being integers, as shown in Fig. 3(b). Note that the pumping laser and cavity field excite the atoms from the ground state to the excited states. The scattering to the α -th state contributes to the susceptibility $f_1^\alpha \equiv |s_\alpha|^2/\varepsilon_\alpha'$. A cavity photon carries a momentum k_c , so only the α_0 -th state with $\alpha_0 = 2L(1 - \gamma_c)$ that matches the cavity mode can be excited, giving a lattice version of Dicke model for noninteracting Bose gas.

When the secondary lattice is added, the momentum distributions of the eigenstates are modified with the appearance of new peaks. For the ground state, additional peaks $\pm 2(k_1 - k_2)$, $\pm 2k_2$ occur between the primary peaks. Accordingly, we show that new momentum peaks of the excited states appear around the peaks of the ground state by the distance $\alpha k_1/L$, see the dashed lines in Fig. 3(c). In this case, besides the α_0 -th state, we find two new excited states that take part in the atom-light scattering process, with $\alpha_1 = 2L(\gamma_c - \gamma)$ and $\alpha_2 = 2L(\gamma_c + 2\gamma - 2)$, see Fig. 3(d). Compared to the α_1 -th state, which is a higher-excited state near the α_0 -th state, the α_2 -th state is located near the low-energy excitation regime, and can dominate the contribution to the susceptibility. As the incommensurate lattice potential increases, more and more peaks arise in the momentum distributions of the ground and excited states, enhancing the contribution to the susceptibility and decreasing the critical pumping of the superradiant transition.

The nontrivial transition is obtained as the disorder strength χ approaches 2, beyond which the eigenstates become localized in real space, but extended in the momentum space, namely, the momentum distribution of each state span the whole momentum space (see the inset of Fig. 3e for a reference). In such a situation, each localized state, including the ground state with energy ε_0 , can be scattered to itself by the cavity field via inducing transition between different momentum components within the localized state. This gives rise to the resonant superradiant scattering. In consequence, the susceptibility $f_1 = \sum_\alpha f_1^\alpha$ diverges due to the contribution from the resonant self-scattering term f_1^0 , for which superradiant instability is induced and the threshold pumping strength vanishes, as shown in Fig. 3(a).

We can find that $\eta_c \equiv 0$ in the whole localized regime. The direct calculation shows that $s_{\alpha\alpha}$ is finite for any localized state as $\chi > 2$ and approaches $\cos(2\pi\gamma_c j_l)$ in the deep localized regime, where j_l is the central site of the localized wavefunction. For a localized state distributing over a few neighboring sites, the coherence of the light scattering by the atoms in such different sites can survive. The backaction of the cavity makes the wavefunction of each state be more localized, giving rise to the

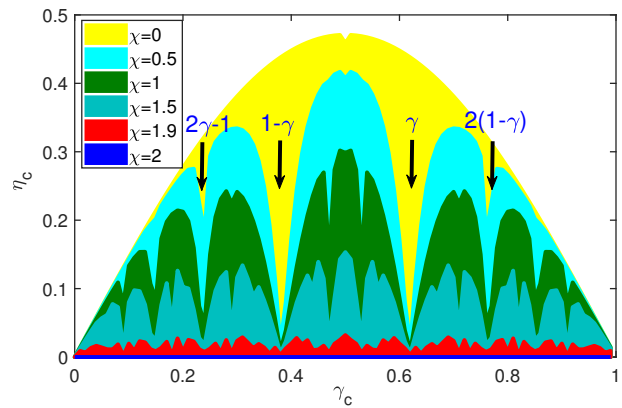


FIG. 4: The diagram of the critical pumping field strength η_c versus γ_c for different disorder strength χ . Here, the parameters are $L = 377$, $N = 100$, $\Delta_c/J = -1$, $\kappa/J = 1$.

self-organization at arbitrarily small pumping strength.

Finally we present in Fig. 4 the dependence of critical pumping field strength η_c on the wave vector of cavity field, as characterized by γ_c , with different disordered potential strengths. When γ_c matches with the disorder potential, i.e. $\gamma_c \sim n\gamma$ or $n(1-\gamma) \pmod{1}$, with n being a positive integer (see the arrows in Fig. 4), the critical pumping strength drops more quickly with the disorder potential. This is because the cavity field enhances the disorder potential. Furthermore, by analyzing carefully the size effect from $L = 300$ to $L = 10000$ sites, we find that the results are size-independent. Note that in real experiment, a weak harmonic potential is needed to trap BEC, which however cannot affect the localization properties substantially [43]. With the Gauss approximation of the Wannier state, $J \sim (V_1/E_R)^{0.75} \exp(-\sqrt{V_1/E_R})$ and $\chi \sim (V_2/E_R) \exp(-1/\sqrt{V_1/E_R})$ with the recoil energy of the prime lattice $E_R = \hbar^2 k_1^2/(2m)$ [46], one can tune χ and J by varying V_2/V_1 .

In conclusion, we have predicted theoretically a novel superradiant instability by coupling the BEC in a localized phase to the cavity, in which the optical pumping threshold for the superradiance vanishes. The localization drives resonant superradiant scattering, in sharp contrast to the extended phases, for which the superradiance phase can occur at a vanishing pumping strength. The prediction is well accessible in the current experiments, and is expected to be valid in the many-body localization regime [53–56] which is achieved once interaction between atoms is included to the present DAA model. This works can open up an intriguing avenue in bridging the studies on the Dicke superradiance and the Anderson localization or many-body localization.

We acknowledge N. R. Cooper and H. Zhai for helpful discussions. This work is supported by the National Natural Science Foundation of China (11875195, 11404225, 11474205, 11504037, 11574008, 11761161003,

11825401), National Key R&D Program of China (2016YFA0301604), and the Research Council (Grant No. MIP-086/2015). Q. Sun and A.-C. Ji also acknowledge the support by the foundation of Beijing Education Committees under Grants No. CIT&TCD201804074 and No. KZ201810028043.

* Electronic address: andrewjee@sina.com

† Electronic address: gediminas.juzeliunas@tfai.vu.lt

‡ Electronic address: xiongjunliu@pku.edu.cn

§ Electronic address: sunqing@cnu.edu.cn

- [1] P. Domokos and H. Ritsch, *J. Opt. Soc. Am. B* **20**, 1098 (2003).
- [2] J. K. Asbóth, P. Domokos, H. Ritsch, and A. Vukics, *Phys. Rev. A* **72**, 053417 (2005).
- [3] D. Nagy, J. K. Asbóth, P. Domokos and H. Ritsch, *Europhys. Lett.* **74**, 254 (2006).
- [4] I. B. Mekhov, C. Maschler and H. Ritsch, *Nat. Phys.* **3**, 319 (2007).
- [5] F. Brennecke, T. Donner, S. Ritter, T. Bourdel, M. Köhl, and T. Esslinger, *Nature* **450**, 268 (2007).
- [6] Y. Colombe, T. Steinmetz, G. Dubois, F. Linke, D. Hunger, and J. Reichel, *Nature* **450**, 272 (2007).
- [7] D. Nagy, G. Szirmai, and P. Domokos, *Eur. Phys. J. D* **48**, 127 (2008).
- [8] H. Ritsch, P. Domokos, F. Brennecke, and T. Esslinger, *Rev. Mod. Phys.* **85**, 553 (2013).
- [9] I. B. Mekhov and H. Ritsch, *J. Phys. B: At. Mol. Opt. Phys.* **45**, 102001 (2012).
- [10] J. Larson, B. Damski, G. Morigi, and M. Lewenstein, *Phys. Rev. Lett.* **100**, 050401 (2008); J. Larson, S. Fernández-Vidal, G. Morigi, and M. Lewenstein, *New J. Phys.* **10**, 045002 (2008).
- [11] S. Gopalakrishnan, B. L. Lev, and P. M. Goldbart, *Nat. Phys.* **5**, 845 (2009); S. Gopalakrishnan, B. L. Lev, and P. M. Goldbart, *Phys. Rev. A* **82**, 043612 (2010); S. Gopalakrishnan, B. L. Lev, and P. M. Goldbart, *Phys. Rev. Lett.* **107**, 277201 (2011).
- [12] P. Strack and S. Sachdev, *Phys. Rev. Lett.* **107**, 277202 (2011); M. Müller, P. Strack, and S. Sachdev, *Phys. Rev. A* **86**, 023604 (2012).
- [13] F. Brennecke, S. Ritter, T. Donner, and T. Esslinger, *Science* **322**, 235 (2008).
- [14] D. Nagy, G. Kónya, G. Szirmai, and P. Domokos, *Phys. Rev. Lett.* **104**, 130401 (2010).
- [15] S. Gupta, K. L. Moore, K. W. Murch, and D. M. Stamper-Kurn, *Phys. Rev. Lett.* **99**, 213601 (2007); K. W. Murch, K. L. Moore, S. Gupta, and D. M. Stamper-Kurn, *Nat. Phys.* **4**, 561 (2008).
- [16] J. Keeling, M. J. Bhaseen, and B. D. Simons, *Phys. Rev. Lett.* **105**, 043001 (2010).
- [17] R. Kanamoto and P. Meystre, *Phys. Rev. Lett.* **104**, 063601 (2010).
- [18] Q. Sun, X.-H. Hu, W. M. Liu, X. C. Xie, and A.-C. Ji, *Phys. Rev. A* **84**, 023822 (2011); Q. Sun, W. M. Liu, and A.-C. Ji, *New J. Phys.* **15**, 013013 (2013).
- [19] B. Padhi and S. Ghosh, *Phys. Rev. Lett.* **111**, 043603 (2013).
- [20] R. Landig, L. Hruby, N. Dogra, M. Landini, R. Mottl, T. Donner, and T. Esslinger, *Nature* **532**, 476 (2016).
- [21] A. U. J. Lode and C. Bruder, *Phys. Rev. Lett.* **118**, 013603 (2017).
- [22] R. H. Dicke, *Phys. Rev.* **93**, 99 (1954).
- [23] F. Dimer, B. Estienne, A. S. Parkins and H. J. Carmichael, *Phys. Rev. A* **75**, 013804 (2007).
- [24] K. Baumann, C. Guerlin, F. Brennecke, and T. Esslinger, *Nature (London)* **464**, 1301 (2010).
- [25] K. Baumann, R. Mottl, F. Brennecke, and T. Esslinger, *Phys. Rev. Lett.* **107**, 140402 (2011).
- [26] R. Mottl, F. Brennecke, K. Baumann, R. Landig, T. Donner, and T. Esslinger, *Science* **336**, 1570 (2012).
- [27] F. Brennecke, R. Mottl, K. Baumann, R. Landig, T. Donner, and T. Esslinger, *Proc. Natl. Acad. Sci. USA.* **110**, 11763 (2013).
- [28] J. Leonard, A. Morales, P. Zupancic, T. Esslinger, and T. Donner, *Nature* **543**, 87 (2017).
- [29] J. Keeling, M. J. Bhaseen, and B. D. Simons, *Phys. Rev. Lett.* **112**, 143002 (2014).
- [30] F. Piazza and P. Strack, *Phys. Rev. Lett.* **112**, 143003 (2014).
- [31] Y. Chen, Z. Yu, and H. Zhai, *Phys. Rev. Lett.* **112**, 143004 (2014).
- [32] J.-S. Pan, X.-J. Liu, W. Zhang, W. Yi, and G.-C. Guo, *Phys. Rev. Lett.* **115**, 045303 (2015).
- [33] D. Yu, J.-S. Pan, X.-J. Liu, W. Zhang, and W. Yi, *Front. Phys.* **13**, 136701 (2018).
- [34] M. R. Bakhtiari, A. Hemmerich, H. Ritsch, and M. Thorwart, *Phys. Rev. Lett.* **114**, 123601 (2015).
- [35] J. Klinder, H. Keler, M. Wolke, L. Mathey, and A. Hemmerich, *PNAS* **112**(11), 3290-3295 (2015).
- [36] W. Zheng and N. R. Cooper, *Phys. Rev. Lett.* **117**, 175302 (2016).
- [37] H. Habibian, A. Winter, S. Paganelli, H. Rieger, and G. Morigi, *Phys. Rev. Lett.* **110**, 075304 (2013).
- [38] L. Zhou, H. Pu, K. Zhang, X.-D. Zhao, and W. Zhang, *Phys. Rev. A* **84**, 043606 (2011).
- [39] K. Rojan, R. Kraus, T. Fogarty, H. Habibian, A. Minguzzi, and G. Morigi, *Phys. Rev. A* **94**, 013839 (2016).
- [40] W. Zheng and N. R. Cooper, *Phys. Rev. A* **97**, 021601(R) (2018).
- [41] S. Aubry and G. André, *Ann. Isr. Phys. Soc.* **3**, 33 (1980).
- [42] G. Roati, C. D'Errico, L. Fallani, M. Fattori, C. Fort, M. Zaccanti, G. Modugno, M. Modugno, and M. Inguscio, *Nature* **453**, 895 (2008).
- [43] E. E. Edwards, M. Beeler, T. Hong, and S. L. Rolston, *Phys. Rev. Lett.* **101**, 260402 (2008).
- [44] Y. Lahini, R. Pugatch, F. Pozzi, M. Sorel, R. Morandotti, N. Davidson, and Y. Silberberg, *Phys. Rev. Lett.* **103**, 013901 (2009).
- [45] L. Fallani, J. E. Lye, V. Guarrera, C. Fort, and M. Inguscio, *Phys. Rev. Lett.* **98**, 130404 (2007).
- [46] M. Modugno, *New J. Phys.* **11**, 033023 (2009).
- [47] G. Modugno, *Rep. Prog. Phys.* **73**, 102401 (2010).
- [48] Y. Lahini, Y. Bromberg, D. N. Christodoulides, and Y. Silberberg, *Phys. Rev. Lett.* **105**, 163905 (2010).
- [49] J. Biddle, B. Wang, D. J. Priour, Jr., and S. Das Sarma, *Phys. Rev. A* **80**, 021603(R) (2009).
- [50] J. Biddle, and S. Das Sarma, *Phys. Rev. Lett.* **104**, 070601 (2010).
- [51] S. Ganeshan, K. Sun, and S. Das Sarma, *Phys. Rev. Lett.* **110**, 180403 (2013).
- [52] M. Larcher, M. Modugno, and F. Dalfovo, *Phys. Rev. A* **83**, 013624 (2011).
- [53] M. Schreiber, S. S. Hodgman, P. Bordia, H. P. Lschen, M.

- H. Fischer, R. Vosk, E. Altman, U. Schneider, I. Bloch, Science, **349**, 6250 (2015).
- [54] S. Ganeshan, J. H. Pixley, and S. Das Sarma, Phys. Rev. Lett. **114**, 146601 (2015).
- [55] H. P. Lüschen, S. Scherg, T. Kohlert, M. Schreiber, P. Bordia, X. Li, S. Das Sarma, and I. Bloch, Phys. Rev. Lett. **120**, 160404 (2018).
- [56] X. Li, X. Li, and S. Das Sarma, Phys. Rev. B **96**, 085119 (2017).